



# Development of eco-friendly GGBS and SF based alkali-activated mortar with quartz sand

Santosh Kumar Karri<sup>1,2</sup> · Markandeya Raju Ponnada<sup>2</sup> · Lakshmi Veerni<sup>3</sup>

Received: 1 March 2022 / Revised: 29 July 2022 / Accepted: 23 August 2022 / Published online: 17 September 2022  
© The Author(s), under exclusive licence to Springer Nature Switzerland AG 2022

## Abstract

To reduce the carbon footprint on the earth, it is a necessity to develop a 100% cement-free mix using pozzolanic binders from industrial wastes. The purpose of the present investigation is to develop 100% cement-free Alkali Activated Slag Mortar (AASM) with binders Ground Granulated Blast Furnace Slag (GGBS) and Silica Fume (SF), with an alkali solution of different combinations of Sodium Silicate ( $\text{Na}_2\text{SiO}_3$ ) and Sodium Hydroxide (NaOH). AASM is developed with different combinations of Binder to the fine aggregate ratio of 1:2, 1:5, and 1:8 with alkaline to binder ratios of 0.5, 0.65, and 0.8. The alkali solutions are established for 9 M, 13 M, 16 M, and 19 M of NaOH and 20%, 35%, and 50% concentrations of  $\text{Na}_2\text{SiO}_3$ . The study is also conducted with different fine-aggregates like river sand, robo sand, quartz sand, and sea sand to establish the suitability of each of them as fine aggregates. The results on different fine aggregates indicate that the quartz sand mixes showed better performance. The results of AASM with different mix combinations reveal 1:2 mix proportion and 0.8 alkali binder ratio mixes exhibiting good performance compared to other mix combinations. 19 M of NaOH and 50% of  $\text{Na}_2\text{SiO}_3$  produce the highest compressive and flexural strength of mortar among the different concentrations of alkali activators solution. SEM and EDX analysis of AASM discloses the formation of strong bond compounds like Calcium-Alumino-Silicate Hydrate (CASH) and Sodium-Alumino-Silicate Hydrate (NASH) are formed resulting in a dense microstructure of AASM, consequently high compressive and flexural strengths are achieved.

**Keywords** Alkali activator · Ground granulated blast furnace slag · Ambient curing · Quartz sand · Micro-structural analysis

## 1 Introduction

The consumption of raw materials like Portland cement for making concrete is increasing every day with the rapid growth of infrastructures [1]. The main application of cement in construction is in the form of mortar or concrete. The mortar strength is directly proportional to concrete strength. As Portland cement is used as a primary binder, the regular usage of cement leads to the cause of 2.8 billion tons of Greenhouse gas released into the atmosphere annually [2].

It is observed that cement production industries are responsible for about 7% of all carbon-di-oxide ( $\text{CO}_2$ ) gas emissions. The Carbon Foot Print is severely affecting the atmosphere and it is estimated that about 1.0 T of  $\text{CO}_2$  are produced for a 1.0 T of clinker in the cement industry [3, 4]. In this context, it is essential to reduce the Carbon Foot Print in the atmosphere. The present generation needs the necessity of replacing the place of cement with eco-friendly materials [1]. Fly ash, GGBS, Rice Husk Ash, Metakaolin, and Silica Fume are waste bi-products from different industries, and in the last two decades research is going on for the proper utilization of the industrial bi-products as a partial replacement of cement [5, 6]. These industrial bi-products which are used for partial replacement of cement are called mineral admixtures. A lot of research has been done on every mineral admixture with partial replacement with cement, and the results showed improved compressive, flexural, split tensile strengths and durability of different concretes [7]. And the strengths of different mineral admixtures depend

✉ Markandeya Raju Ponnada  
markandeyaraju@yahoo.com

<sup>1</sup> JNTU Kakinada, Kakinada, AP, India

<sup>2</sup> Department of Civil Engineering, MVGR College of Engineering (A), Vizianagaram, AP, India

<sup>3</sup> Department of Civil Engineering, University College of Engineering (A), JNTU Kakinada, Kakinada, AP, India

on the constituents present in the admixture and the amount of replacement [8, 9].

Now the research is going on the complete replacement of cement to mitigate the impact of cement on the global environment [10]. This has led to the development of alkali-activated mortar/concrete with a combination of some industrial by-products along with alkali activators [11]. The commonly used alkali activators are the mixture of sodium based NaOH & Na<sub>2</sub>SiO<sub>3</sub> or potassium-based KOH & K<sub>2</sub>SiO<sub>3</sub> [12]. In alkali-activated mortar/concrete, the binding compounds are produced by alkali activation of alkali activators with calcium, silicon, aluminium, and ferrous sources materials like GGBS, silica fume, metakaolin, rice husk ash (RHA), and fly ash [13]. From Table 1 it is observed that the source material should be rich in calcium (Ca), silica (Si) and alumina (Al) could make potential alkali-activated mortar/concrete [12, 14].

GGBS plays a very vital role as a binder in the matrix. The bonding of GGBS with Fine aggregate also plays a very important role in mortar as fine aggregate occupies more volume. The alternate fine aggregates such as manufactured sand, quartz sand, sea sand, and artificial sands replace the need for river sand which is a stressed natural resource. The study on the effect of the replacement of different alternate binders and different alternate fine aggregates on the properties of mortars and concrete is very important [15]. The performance of GGBS is observed to be very good along with different alternate fine aggregates [16]. The partial replacement of GGBS with cement does not adversely affect the performance of fresh mortar/concrete in terms of properties like workability, flowability, and hardened properties with artificial and other alternate aggregates [17, 18]. The concrete/mortar performance is also observed to be reasonably good with partial and complete replacement of cement with GGBS in different special concretes like geopolymer concrete and alkali activated concretes, etc. [19, 20]. The XRD, SEM, and EDS analysis revealed that there is a better

formation of end products that enhance the strength with GGBS as a binder than other alternate binders [21].

The study on the feasibility of the special mortars/concretes is very important as the ingredients are waste materials or industrial byproducts mixed in different proportions. GGBS, fly ash, silica fume, metakaolin and other alternate cementitious material based geopolymer concretes and alkali activated concretes have to be thoroughly studied for their feasibility in the construction field with different aggregates [22–24]. GGBS based mortar/concrete exhibited significant improvement in environmental sustainability due to its minimal environmental and economic impact [25].

Alkali activated slag mortar (AASM) is an advanced and eco-friendly special mortar unlike Geopolymer mortar and manufactured by complete replacement of cement with GGBS. In alkali-activated mortar/concretes, the binders are strengthened after alkali activation because of activators. The study of alkalis on GGBS mortars has been initially developed by A.O. Purdon in 1940 [26].

Alkali activation is a process that occurs in the presence of an alkaline medium with a binder material that results in an ionic composition with good bonding. The alkaline medium is Sodium or Potassium Hydroxides (NaOH or KOH) and Sodium or Potassium Silicates (Na<sub>2</sub>SiO<sub>3</sub> or K<sub>2</sub>SiO<sub>3</sub>) [27]. The higher the concentration of alkali accelerates the reactants in the chain mechanism and leads to a quicker reaction [28]. Na<sub>2</sub>SiO<sub>3</sub> is considered to be a more active activator to develop strength development compared to K<sub>2</sub>SiO<sub>3</sub> and Na<sub>2</sub>CO<sub>3</sub>.

The alkali activation process in terms of polymeric reactions is explained by Davidovits [29]. The compounds formed due to alkali activation are observed to develop high mechanical properties for these mixes. After alkali activation, the chemical formula for the compound formed is  $M_n(\text{Si-O})_z[-\text{Al-O}]_n \times w\text{H}_2\text{O}$ , where  $M$  represents an alkaline element,  $-$  represents the bond between elements,  $n$  is the degree of alkalination, and  $z$  is 1, 2, or 3 based on the number of connections [30].

Hua Xu studied the causes for the high strength in AASM for optimum percentages of CaO, K<sub>2</sub>O, and the Si–Al bond, the kind of alkali, and the ratio Si/Al in the mix [12]. In AASM, the ratios SiO<sub>2</sub>/Al<sub>2</sub>O<sub>3</sub>, R<sub>2</sub>O/Al<sub>2</sub>O<sub>3</sub>, and SiO<sub>2</sub>/R<sub>2</sub>O; (R = Na+ or K+) significantly affect the development of the binder structure, mechanical properties, and durability of binders. The compressive strength and SiO<sub>2</sub>/R<sub>2</sub>O ratio indicate an increase in alkali (Na or K) content or reduction in silicate content that is responsible for the increase in the mechanical strength of concrete. They also indicate the formation of Alumino-Silicate network structures [12, 31, 32].

The major primary product formed in the Portland cement hydration reaction is a C-S-H-type gel. The secondary products formed may be ettringite (hydrated calcium aluminium sulfate hydroxide), calcium aluminate mono-sulfate hydrate,

**Table 1** Chemical composition of cement, fly ash, GGBS, silica fume (wt%)

Constituents	Cement	Fly ash	GGBS	Silica fume
CaO	63.87	21	42.26	0.89
SiO <sub>2</sub>	20.62	37	34.24	93.17
Al <sub>2</sub> O <sub>3</sub>	4.87	9.89	13.75	0.14
Fe <sub>2</sub> O <sub>3</sub>	3.35	4.45	1.10	0.04
SO <sub>3</sub>	2.5	1.91	0.24	0.004
MgO	1.54	3.5	5.88	0.51
K <sub>2</sub> O	–	–	0.32	2.01
Na <sub>2</sub> O	–	0.56	0.28	0.58
LOI	1.5	3.12	0.72	2.43

and portlandite (calcium hydroxide) [33]. Similarly, in alkali-activated mortar/concrete also the alkali activation from primary and secondary products, the products developed are based on the constituents of source material, their reaction, and curing condition. The alkali activation of the calcium-rich binder with sodium hydroxide from primary products like Calcium-Alumino-Silicate Hydrate (CASH) and Sodium-Alumino-Silicate Hydrate (NASH) compounds like C-S-H and also other secondary compounds depend on the type and amount of activator used, composition, and the curing conditions [34]. The source materials for the alkali-activated mortar may be GGBS, Fly Ash, Rice Husk Ash, Metakaolin, and Silica Fume. Any of these materials individually or in combinations may form a strong binder after alkali activation [7].

The alkali activators NaOH or KOH can initiate alkali activation of binders [35, 36], but maximum researchers adopt both NaOH and  $\text{Na}_2\text{SiO}_3$  for a better alkali Activation process [19, 37, 38]. Compressive strength reduces with the increase of alkaline content from 35 to 45% of the total binder. Variation of  $\text{Na}_2\text{SiO}_3$  to NaOH affects the performance of mortar/concrete. The best ratio of  $\text{Na}_2\text{SiO}_3$  to NaOH for GGBS based alkali activated mortar is 2.5. The workability and setting time increased increase in alkaline liquid content [39].

Maximum works on alkali activated mortars are performed on fly ash and GGBS based mortars/concretes [19, 40, 41], and few works are available with the combination of GGBS and SF [37]. The GGBS alkali activated concretes are producing early age strengths, high compressive strengths, and good durability performance [19, 42].

## 2 Objective

Tremendous work has been done on alkali-activated concrete across the world. There is a scarceness of study in the available literature on the effect of alkali activator concentration on the combination of various suitable pozzolanic binders with the incorporation of different fine aggregates as sand. The objective of this work is to study the most suitable combination of binders that can be used in alkali-activated mortar, identification of the suitable type of fine aggregate, and the influence of alkali activators on the binder. The microstructural analysis of the best proportion of AASM is also performed.

## 3 Methodology for the development of AASM

Locally available materials with rich calcium, silica, and aluminum are the most suitable source materials for making AASM. The choice depends on various factors such as availability, feasibility, cost, literature, type of application,

and specific demand of the end-users. Figure 1 represents the flow chart of the methodology adopted in this experimental study on AASM. To identify the best binder combination among GGBS and SF, a total of 16 mixes are carried out, and for each mix three cubes are cast for 7 days of ambient air curing. To study the different fine aggregates on river sand, robo sand, quartz sand, and sea sand total of 24 mixes are carried out and for each mix six cubes are cast for seven and 28 days of curing. To develop AASM for different mix combinations and parameters, a total of 108 combinations are adopted. For each mix combination, nine cubes are cast for 7, 28, and 56 days of ambient air curing to study the Workability of fresh AASM, compressive strength, and flexural strength tests on hardened concrete are carried out after 28 days of ambient air curing.

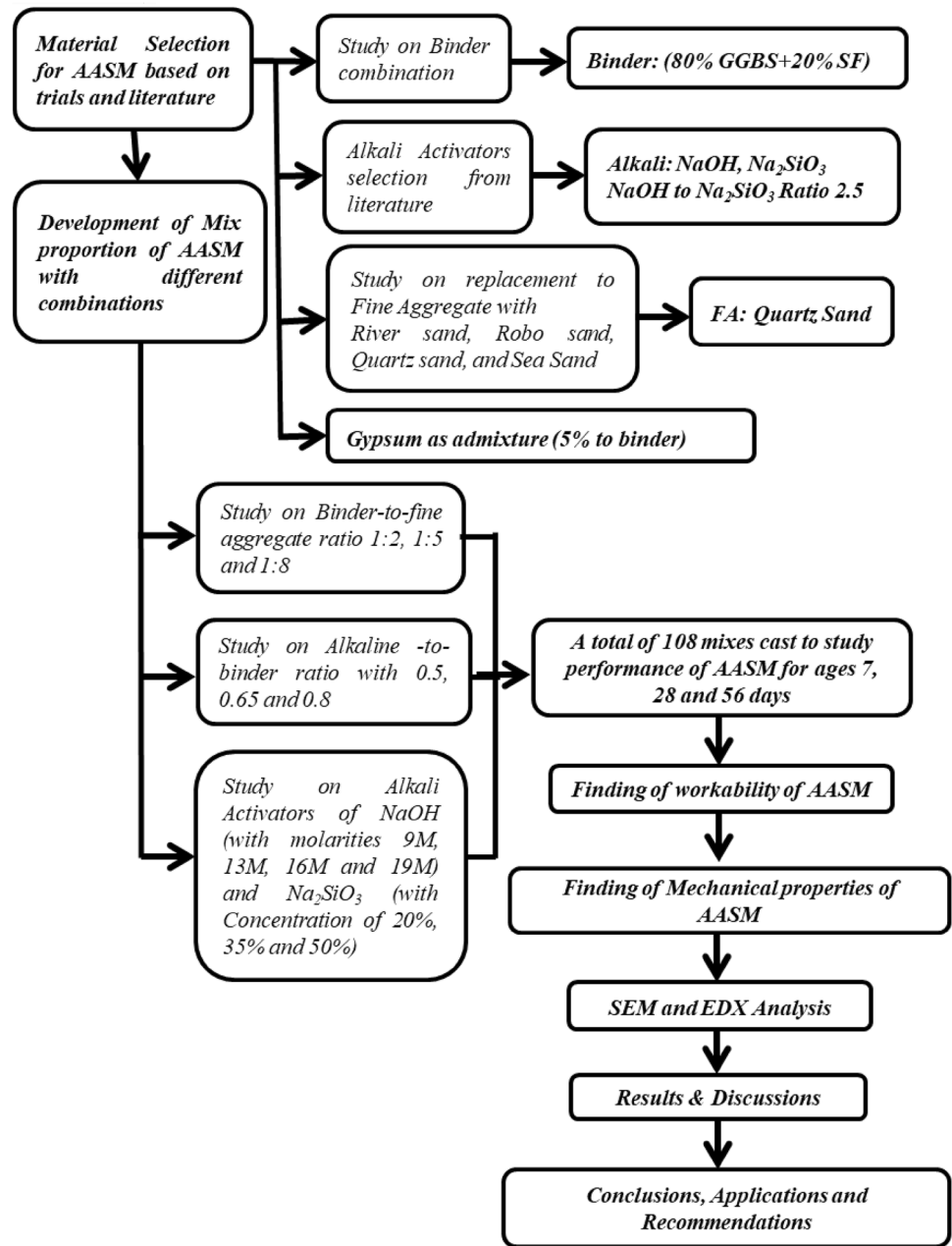
### 3.1 Binders

For making AASM, binders that are generally used as supplementary cementitious materials are adopted. These are different from OPC due to their latent hydraulic properties. Among the various industrial by-products adopted for making AAM, the production of one-ton GGBS releases only 0.07 tons of  $\text{CO}_2$  whereas the cement process produces 0.95 tons of  $\text{CO}_2$  [43]. As shown in Table 1, the GGBS is obtained from a by-product of the iron manufacturing industry, which is rich in Calcium, Aluminium, and a moderate percentage of Silica [44]. To obtain the perfect binder for AAM the GGBS which contains a moderate percentage of silica should be balanced with rich silica material [45, 46]. Silica Fume (SF) also known as micro silica contains rich silica of around 93% and it is obtained from the manufacturing of silicon alloy industries [23, 24].

### 3.2 Alkali solution

The alkaline solution made with NaOH and  $\text{Na}_2\text{SiO}_3$  is used for the alkalination of the binder [36]. Soluble silicate with the presence of alkaline hydroxides produces a higher rate of reaction and also enhances the reaction with the source material. The ratio of alkali activators  $\text{Na}_2\text{SiO}_3/\text{NaOH}$  significantly alters the reaction and final gel formation. In general, the alkali ratio for different mix designs is varying from 1.0 to 2.5 [47]. For this study, the ratio  $\text{Na}_2\text{SiO}_3/\text{NaOH}$  is considered 2.5 [48]. From trial studies, the NaOH molarities are generally considered from 9 to 19 M. For Molarity less than 9, the strengths are not as desirable. For Molarity greater than 19, the mix is very stiff and sets very Quickly. So, the range of molarity is considered from 9 to 14 M. Also, there will be a long gap of division (i.e. 6), if 9 M, 14 M, and 19 M concentrations considered over a range of 10 M are only studied. This may not give a broad idea of the effect of NaOH concentration on the properties of concrete. To

**Fig. 1** The methodology adopted for the development of AASM



study more concentrations over the range, the final NaOH molarities considered are 9 M, 13 M, 16 M, and 19 M (4 concentrations).

### 3.3 Fine aggregate

The most preferred choice and largely used fine aggregate for construction purposes is natural river sand. The scarcity of river sand is an important challenge faced by the construction industry in recent years. A lot of literature on the replacement of various materials with natural sand in concrete is available[49]. The most common of these types of fine aggregates are river sand, robo sand, quartz sand, and

sea sand. Currently, many researchers are working on the suitability of sea sand for construction [50]. The preliminary results showed quartz sand performance is good compared to other sands. Quartz sand is a type of manufactured sand from quartzite quarry. The crushed large quartz stones to finer particles of less than 4.5 mm are used as fine aggregate in this study[51].

### 3.4 Gypsum

AASM sets very quickly during the process of mixing and making cubes, so AASM mix needs a retarder that can increase the setting time. Gypsum is an admixture that can

be used as an excellent retarder. To meet the desired setting qualities in the finished product, a certain amount of gypsum is needed to add. Based on trails a quantity of 5% of gypsum to binder content is good for the desired setting time and the excess use of gypsum may cause unwanted expansion and indefinite delay in the setting of concrete.

### 3.5 Ambient air curing

Alkali activated mortars/concretes can be cured in different curing conditions like a conventional method of immersion in water, oven curing at elevated temperatures, and ambient air curing [52–54]. But the preferred curing regime for fly ash based Alkali Activated concretes is oven curing at elevated temperature as it ensures complete alkali activation [10, 55], whereas ambient air curing is the most suitable curing regime for alkali activated concretes with GGBS [48, 56]. The ambient air curing regimes are producing high compressive strength results for alkali activated slag mortars/concretes. And also water is scarce around the world, and ambient air curing is advised. So ambient air curing regime is adopted for the development of AASM.

### 3.6 Assessment of optimum binder combinations

To study the required combination percentages of GGBS to SF binders, various percentages such as 100–0%, 80–20%, 60–40%, and 40–60% are considered using a binder to fine aggregate mix proportion of 1:3 along with the alkali to Binder ratio of 0.8. The river sand is used as the fine aggregate for all the combinations studied. Table 2 illustrates the various proposed trial mixes for alkali solutions of 9 M and 14 M NaOH with a 50% concentration of Na<sub>2</sub>SiO<sub>3</sub>. Total of 16 trial mixes (3 cubes for each mix) of 70.7 × 70.7 × 70.7 mm<sup>3</sup> size mortar cubes are cast and tested for compressive strength after 7 days of ambient air curing.

Figure 2 represents the compressive strength results obtained for various combinations of GGBS and SF mortar cubes at 7 days of ambient curing. The results show that 80% of GGBS + 20% of SF combination achieved high compressive strengths as compared to other combinations for both 9 M and 14 M of NaOH. For the same combination/percentage of binder, the compressive strength of the 14 M trial mix is found to be 18.2% higher than that of the 9 M trial mix.

### 3.7 The optimum dosage of gypsum

During the initial trials, it is observed that the AASM cubes are subjected to a quick setting with 80% of GGBS and 20% of SF. So it is necessary to increase the setting time for ease of application on-site within a stipulated time. Gypsum and some standard superplasticizers are very good retarders to increase the setting time. However, gypsum is observed to be better than superplasticizers. So, the optimum dosage of gypsum required for a convenient set is required [57, 58]. The following mix details are considered to find the optimum percentage of gypsum to the binder content.

- Binder (GGBS: SF) = 4:1
- Mix proportion (Binder: Fine aggregate (river sand)) = 1:5
- Alkali solution: binder = 0.6
- Percentages of gypsum to binder = 1%, 3%, 5%, and 7%
- Concentration of NaOH = 9 M, 14 M
- Concentration of Na<sub>2</sub>SiO<sub>3</sub> = 50%
- Age and type of curing = 28 days of ambient air curing

Calorimetric tests to determine the optimum concentration of the gypsum in the mix may not be possible as the mix is amorphous in nature. Further, the mix is expected to be used for making mass concrete or reinforced concrete and minor changes in concentration may not affect the setting performance of the mix significantly.

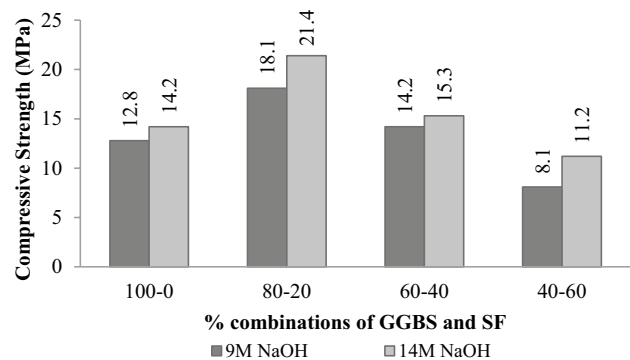


Fig. 2 Compressive strengths of mortar cubes for different combinations of GGBS and SF after 7 days

Table 2 Mix proportion and combinations for GGBS and SF

Mix proportion	1:3				1:3				
Molarity (M)	9				14				
Na <sub>2</sub> SiO <sub>3</sub> (%)	50				50				
A/B	0.8				0.8				
Binder	GGBS (%)	100	80	60	40	100	80	60	40
	SF (%)	0	20	40	60	0	20	40	60



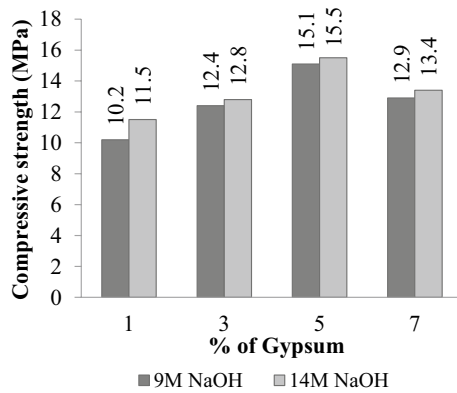


Fig. 3 Compressive strengths of mortar cubes for different % of Gypsum after 28 days

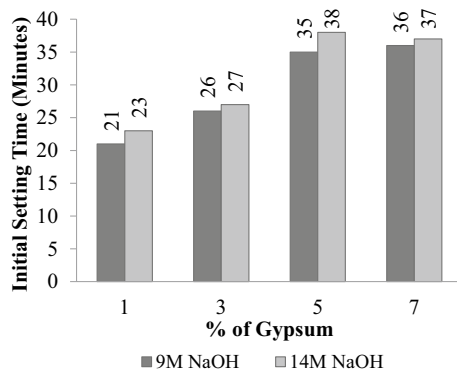


Fig. 4 Initial setting time of mortar mix for different % of Gypsum after 28 days

From Figs. 3 and 4 represents compressive strength and initial setting time values for different % of gypsum (1%, 3%, 5%, and 7%). According to IS 4031-part 5, the Initial setting time should not be less than 30 min. From the results, the performance of AASM is good at 5% gypsum for both initial setting time and compressive strength point of view. Therefore 5% of gypsum is used as a binder for the entire study.

### 3.8 Ascertainment of suitable fine aggregate for AASM

To establish the suitability of different fine aggregates for developing AASM, a study is conducted with river sand, quartz sand, robo sand, and sea sand with a 1:3 mix proportion as depicted in Table 3. Total forty-eight combinations of AASM mixes are prepared and tested under ambient curing for 7 and 28 days respectively.

Figures 5 and 6 represent the compressive strengths of different sands for varying NaOH and Na<sub>2</sub>SiO<sub>3</sub> after 7 and 28 days respectively for a 1:3 mix proportion. The results show that the Quartz sand performance is better for all combinations of NaOH and Na<sub>2</sub>SiO<sub>3</sub>. Both river sand and manufactured sand exhibited similar performance with the effect of alkali solution and low performance is observed for sea-sand type mixes. It is evident from Figs. 3 and 4 that among all combinations, mixes containing quartz-sand showed better performance compared to others.

Table 3 Combinations of alkali solutions along with other parameters

Alkali solutions	Mix proportion	% of Na <sub>2</sub> SiO <sub>3</sub>	Molarities of NaOH	Age (days)	Alkali binder ratio	Fine aggregate
Na <sub>2</sub> SiO <sub>3</sub> and NaOH	1:3	20, 50	9, 14, 19	7 and 28	0.8	River sand, quartz sand, robo sand, sea sand

Fig. 5 Compressive strengths of different sands for varying NaOH and Na<sub>2</sub>SiO<sub>3</sub> after 7 days

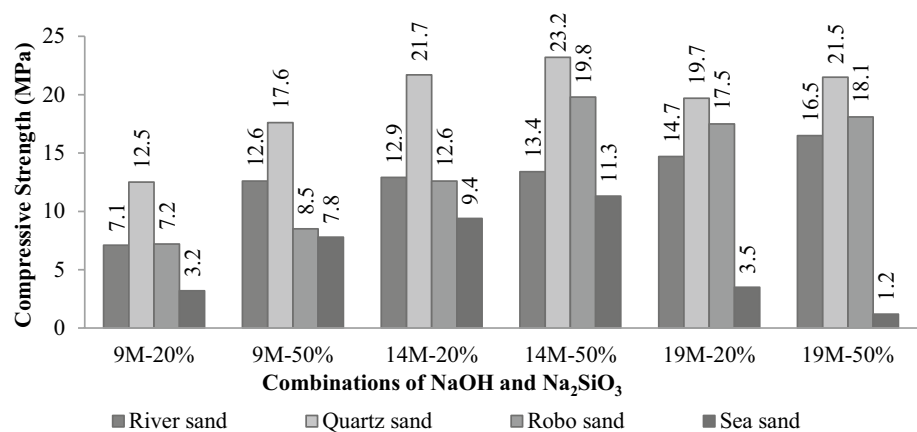
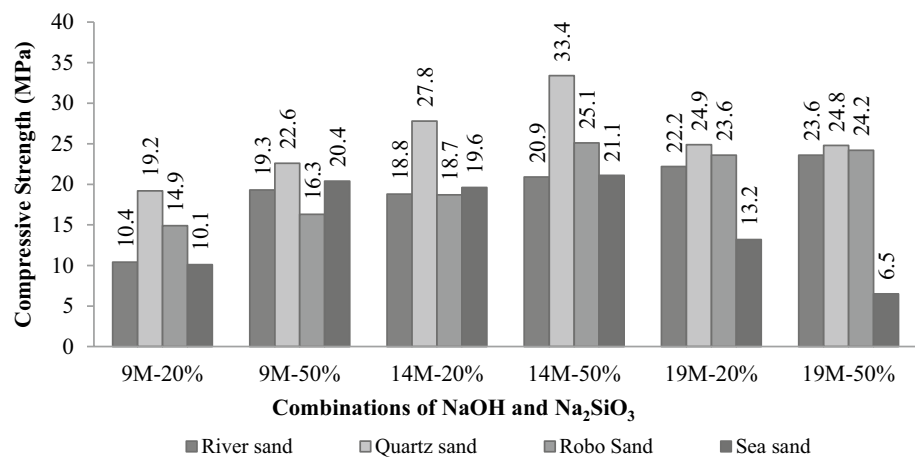


**Fig. 6** Compressive strengths of different sands for varying NaOH and Na<sub>2</sub>SiO<sub>3</sub> after 28 days



### 3.9 Development of AASM for different combinations of alkalis with quartz sand

From the above studies, the following mix proportions and parameters are considered for the development of AASM and studied the effect of alkalis on binder.

Binder (GGBS:SF) = 4:1

Mix proportion (binder:fine aggregate (quartz sand)) = 1:2, 1:5, 1:8

Alkali solution: binder = 0.5, 0.65, 0.8

The concentration of NaOH = 9 M, 13 M, 16 M, 19 M

The concentration of Na<sub>2</sub>SiO<sub>3</sub> = 20%, 35%, 50%

Age and type of curing = 7, 28, and 56 days of ambient air curing

Gypsum = 5% to binder is added to the mix (to control the setting time).

### 3.10 Mix calculation

For different combinations of AASM developed using the above mix proportion and parameters, mix calculations are carried out for cubes of size 70.7 mm × 70.7 mm × 70.7 mm (for compressive strength) and square prisms of size 160 mm × 40 mm × 40 mm for flexural tensile strength.

A total of 108 combinations are carried out for this study. For workability also, mix calculations are carried out for frustum cone of size 100 mm bottom internal diameter, 70 mm top internal diameter, and height 50 mm.

For each combination, nine cubes are cast for testing of compressive strength at the age of 7, 28, and 56 days, and a total of 972 samples are prepared for the compressive test. For each combination, three square prisms are cast for testing flexure strength at the age of 28 days and prepared a total of 324 samples for the flexure test. Table 4 represents the quantities of materials of AASM per m<sup>3</sup> mortar in 1:2, 1:5, and 1:8 mix proportions.

The quantities for different molarities of NaOH are calculated based on a table given for estimating the quantities of water and hydroxide solids in Perry's Handbook which is the standard reference book published in 1915 by Prof. Perry [59].

### 3.11 Preparation of mortar specimens

Based on the quantities from mix calculations AASM, cubes of size 70.7 × 70.7 × 70.7 mm<sup>3</sup> as per IS: 2250 1981 and IS: IS: 4031(6) 1988 for the compressive test [60, 61] and square prisms of size 160 mm × 40 mm × 40 mm are prepared as per ASTM C348-21 for flexural strength [62]. First, the binder (GGBS and SF), Quartz sand, and gypsum are mixed thoroughly. Gypsum is added to the mix to control the fast setting of the mortar. Separate solutions of NaOH and Na<sub>2</sub>SiO<sub>3</sub> are prepared 1 h before mixing with the binder [63]. For the preparation of Alkali solution, NaOH of required molarity is prepared based on Perry's Handbook, and Na<sub>2</sub>SiO<sub>3</sub> is prepared based on the percentage concentration required [59]. After 1 h of resting of alkali solution, they are added to the binder and mixed thoroughly. For making the Alkali activated slag mortars and concretes developed by the majority of researchers, Alkali activators are to be prepared 24 h ahead of mixing. This is one of the practical difficulties in the application of these mortars and concretes in the construction industry. However, the Alkali activated slag mortar and concrete developed and presented in this paper require the Alkali

**Table 4** Quantities of binder and fine aggregate of AASM in kg/m<sup>3</sup>

Mix	GGBS	Silica fume	Gypsum	Quartz
1:2	532.00	133.00	35.00	1400.00
1:5	266.00	66.50	17.50	1750.00
1:8	177.33	44.33	11.67	1866.65

activators to be prepared 1 h ahead of mixing. This is a great advantage in terms of the application of this mix in the construction industry. However, unlike regular water used to mix in mortar/concrete, the usage of alkali activators generates a lot of heat and hence has some practical impacts/difficulties while mixing. However, they can be overcome by using skilled labor.

The workability test for each mix as per IS: 5512 1983 using the Flow table is determined. The fresh mortar mix is placed in cube moulds and prism moulds and compacted using a vibrating machine as per IS: 10080 1982 [64]. After demolding, the cube specimens are kept in air for ambient curing for 7, 28, and 56 days and tested for compressive strength. The prism specimens are kept in the air for ambient curing for 28 days and tested for flexure strength. The preparation of the AASM mix, flow test, and casting of mortar cube and specimens are shown in Figs. 7A,B, 8A,B and 9A,B.

## 4 Results and discussions

A total of 108 mixes have been considered based on preliminary studies for different mix proportions of 1:2, 1:5, and 1:8 with A/B ratios of 0.5, 0.65, and 0.8, and the notations (Mix ID) for those AASM mixes are presented in Table 5. The workability of these 108 mixes of AASM is determined by conducting a flow test. The water absorption test is also conducted to know the volume of pores. Compressive strength and flexural strength tests are conducted on the mortar cube and prism specimens to know the mechanical properties of the 108 mixes.

### 4.1 Workability of AASM

The workability on fresh AASM of 108 mixes is experimentally determined as per IS: 5512 1983 using a flow table that is used for testing hydraulic cement and pozzolanic materials [65–67]. The flow table apparatus contains a round table

**Fig. 7** **A** AASM cubes in ambient air, **B** cube compression test

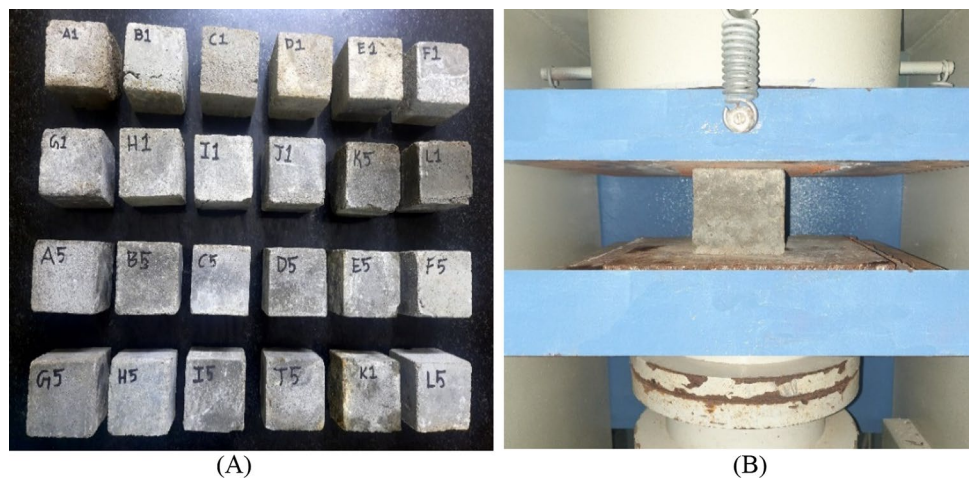


**Fig. 8** **A** Flow test on AASM mixture, **B** Flow value measurement of AASM

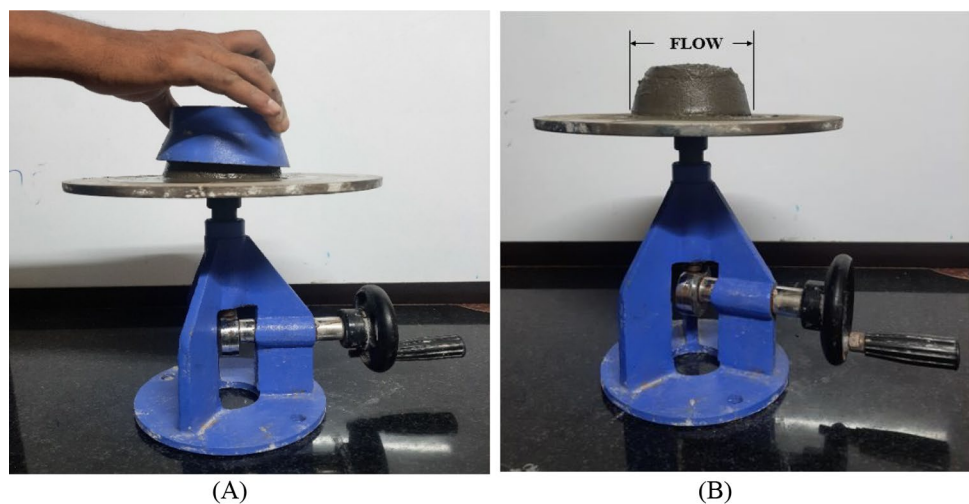




**Fig. 9** **A** Prism specimens of AASM mix. **B** Flexure test on AASM prism

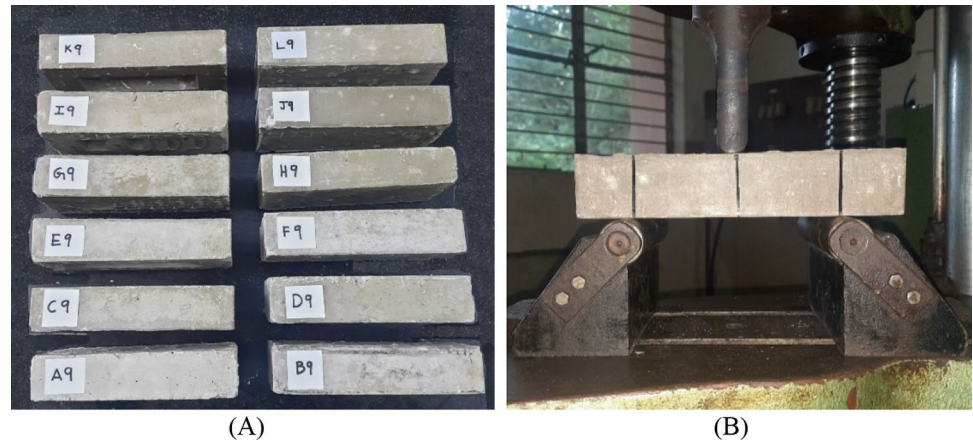


**Table 5** Notation adopted for various AASM mixes

Mix parameters	20	20	20	35	35	35	50	50	50	Na <sub>2</sub> SiO <sub>3</sub> (%)	
Mix	NaOH (M)	0.5	0.65	0.8	0.5	0.65	0.8	0.5	0.65	0.8	A/B ratio
1:2	9 M	A1	A2	A3	A4	A5	A6	A7	A8	A9	Mix notation
	13 M	B1	B2	B3	B4	B5	B6	B7	B8	B9	
	16 M	C1	C2	C3	C4	C5	C6	C7	C8	C9	
	19 M	D1	D2	D3	D4	D5	D6	D7	D8	D9	
1:5	9 M	E1	E2	E3	E4	E5	E6	E7	E8	E9	
	13 M	F1	F2	F3	F4	F5	F6	F7	F8	F9	
	16 M	G1	G2	G3	G4	G5	G6	G7	G8	G9	
	19 M	H1	H2	H3	H4	H5	H6	H7	H8	H9	
1:8	9 M	I1	I2	I3	I4	I5	I6	I7	I8	I9	
	13 M	J1	J2	J3	J4	J5	J6	J7	J8	J9	
	16 M	K1	K2	K3	K4	K5	K6	K7	K8	K9	
	19 M	L1	L2	L3	L4	L5	L6	L7	L8	L9	

with a diameter of 250 mm, which is resting on a vertical shaft and supporting frame, and a frustum cone with a base diameter of 10 mm. The frustum of the cone is placed on the Flow table apparatus and mortar is filled into it in three layers tamping 25 blows on each layer uniformly. The cone frustum should be removed from the table after filling of mortar mix. 25 drops are applied to the table on which fresh mortar is placed in the shape of a cone frustum. The spread of the mortar on the table referred to as the Flow value is then measured. This flow value generally varies from 10 to 25 cm. A flow value of 25 represents high workability and a flow value of 10 represents very low workability of mortar. Table 6 represents the flow values of different AASM mixes.

From the results, the 1:2 mix proportion is having good workability compared to the 1:5, and 1:8 mix proportions. A Higher A/B ratio mixes are producing very high workability compared to low A/B ratio mixes. Alkali activators are also affecting the workability, as the concentration of Na<sub>2</sub>SiO<sub>3</sub> increasing, the workability is decreasing, and as the molarity of NaOH increases the workability also increases. For the mix with 0.8 A/B ratios and the 50% concentration of

Na<sub>2</sub>SiO<sub>3</sub> low value of workability is observed even for the high A/B ratio.

### 4.2 Water absorption of AASM

To know the pore size distribution in mortar specimens Porosimetry and water absorption tests are used. In this study, water absorption tests are conducted to know the presence of voids in AASM specimens. The AASM cube specimens of size 70.7mm × 70.7 mm × 70.7 mm are kept in water for 24 h at room temperature. They are taken out from the water and the surface of the cube is cleaned and saturated weight is recorded as W<sub>s</sub>. These samples are placed in an oven at a temperature of 100 °C for 5 h and their weight is recorded as W<sub>D</sub>. Using these weights, water absorption is calculated by the equation.

$$\% \text{ of water absorption} = (W_s - W_D) \times 100 / W_D.$$

A water absorption test is used to know the presence of pores in mortar specimens. If the percentage of water

**Table 6** Flow values of different mixes of AASM

Mix parameters			A/B ratio	0.5	0.65	0.8	0.5	0.65	0.8	0.5	0.65	0.8
			Na <sub>2</sub> SiO <sub>3</sub> (%)	20	20	20	35	35	35	50	50	50
Mix	NaOH (M)	Mix notation	1	2	3	4	5	6	7	8	9	
1:2	9 M	A	10	15	25	10	14	25	10	13	16	
	13 M	B	10	15	25	10	14	25	10	13	16	
	16 M	C	10	16	25	10	15	25	10	14	18	
	19 M	D	11	16	25	10	16	25	10	15	19	
1:5	9 M	E	10	13	25	10	13	25	10	13	16	
	13 M	F	10	13	25	10	13	25	10	13	16	
	16 M	G	10	12	25	10	14	25	10	14	17	
	19 M	H	11	13	25	10	13	25	10	14	17	
1:8	9 M	I	10	11	20	10	13	25	10	13	16	
	13 M	J	10	11	20	10	13	25	10	13	16	
	16 M	K	10	12	21	10	14	25	10	13	16	
	19 M	L	10	12	21	10	15	25	10	14	17	

Flow values of AASM in cm

absorption is more, it represents the presence of more pores in the specimen. Table 7 represents the percentage of water absorption of different AASM mixes.

From the water absorption results of AASM, it is observed that the percentage of water absorption of the mix proportion of 1:8 is more and this means that there are more voids. The *A/B* ratio also affects water absorption. As *A/B* increases the water absorption decreases. So a high *A/B* ratio decreases the pores. The alkali activators also affect water absorption. It is observed that the increasing molarity of NaOH decreases the water absorption percentage. but with the increase of Na<sub>2</sub>SiO<sub>3</sub> concentration, the water absorption percentage increases.

### 4.3 Compressive strength of AASM

The compressive strength is a very important mechanical property of mortar/concrete. So compressive strength of AASM of Mix proportions 1:2, 1:5, and 1:8 at different ages of 7, 28, and 56 days of ambient air curing are studied and the results for different alkali concentrations are presented in Fig. 10A–L.

### 4.4 Flexure strength of AASM

To study the mechanical property of AASM flexure strength is also important along with compressive strength [68, 69]. Flexural strength test is conducted on AASM mix prisms of Mix proportions 1:2, 1:5, and 1:8 at 28 days of ambient air

**Table 7** Water absorption of different mixes of AASM

Mix parameters			A/B ratio	0.5	0.65	0.8	0.5	0.65	0.8	0.5	0.65	0.8
			Na <sub>2</sub> SiO <sub>3</sub> (%)	20	20	20	35	35	35	50	50	50
Mix	NaOH (M)	Mix notation	1	2	3	4	5	6	7	8	9	
1:2	9 M	A	3.7	8.9	5.4	10.1	2.6	9.3	16.8	3.8	11.5	
	13 M	B	2.8	1.1	0.9	0.6	0.9	0.8	10.3	0.8	1.6	
	16 M	C	0.9	0.9	0.7	0.6	0.6	0.9	1.1	0.6	0.9	
	19 M	D	1.2	0.8	0.6	0.2	0.5	0.3	0.6	0.8	0.5	
1:5	9 M	E	14.7	9.7	4.3	18.8	11.7	14.6	18.7	12.4	11.7	
	13 M	F	9.9	3.0	1.4	12.1	4.2	3.8	11.7	7.8	3.4	
	16 M	G	9.2	2.9	0.9	14.5	9.6	8.2	16.5	10.8	5.7	
	19 M	H	4.9	0.8	0.9	9.9	1.7	3.2	9.7	4.8	0.9	
1:8	9 M	I	20.9	18.9	16.9	20.7	18.7	14.9	20.7	18.5	16.2	
	13 M	J	20.3	16.7	11.8	20.8	17.2	12.7	20.6	18.9	13.2	
	16 M	K	18.7	16.2	12.8	19.0	17.0	14.0	20.8	18.6	14.8	
	19 M	L	15.9	12.7	11.6	19.1	14.0	12.6	18.9	17.0	11.7	

Water absorption of AASM in %

**Fig. 10** **A** Compressive strengths of AASM of 1:2 mix and 9 M of NaOH, **B** Compressive strengths of AASM of 1:2 mix and 13 M of NaOH, **C** Compressive strengths of AASM of 1:2 mix and 16 M of NaOH, **D** Compressive strengths of AASM of 1:2 mix and 19 M of NaOH, **E** Compressive strengths of AASM of 1:5 mix and 9 M of NaOH, **F** Compressive strengths of AASM of 1:5 mix and 13 M of NaOH, **G** Compressive strengths of AASM of 1:5 mix and 19 M of NaOH, **H** Compressive strengths of AASM of 1:8 mix and 9 M of NaOH, **I** Compressive strengths of AASM of 1:8 mix and 13 M of NaOH, **J** Compressive strengths of AASM of 1:8 mix and 16 M of NaOH, **K** Compressive strengths of AASM of 1:8 mix and 19 M of NaOH, **L** Compressive strengths of AASM of 1:8 mix and 19 M of NaOH

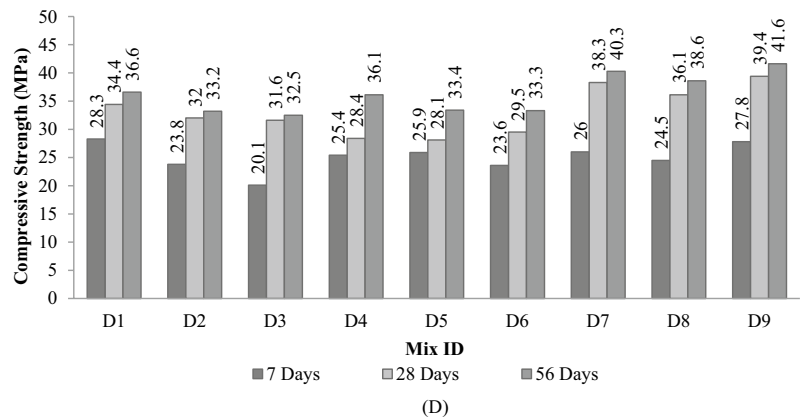
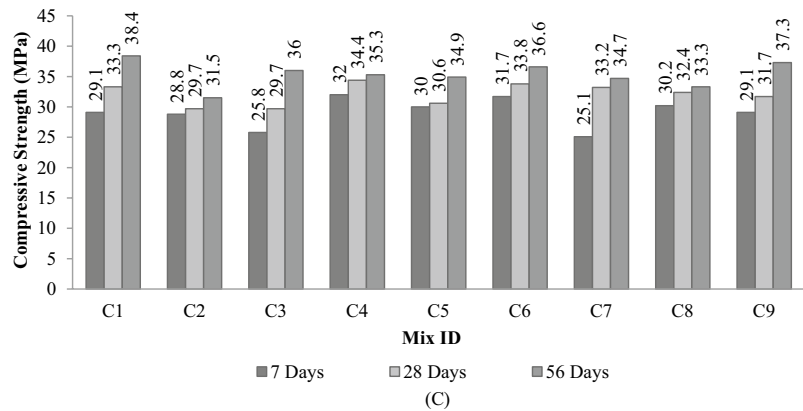
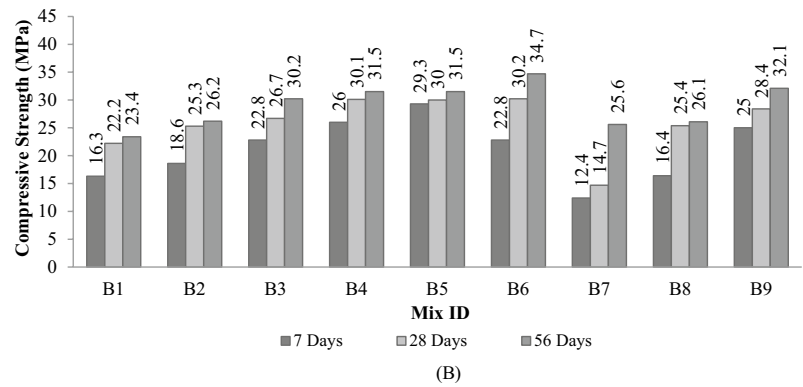
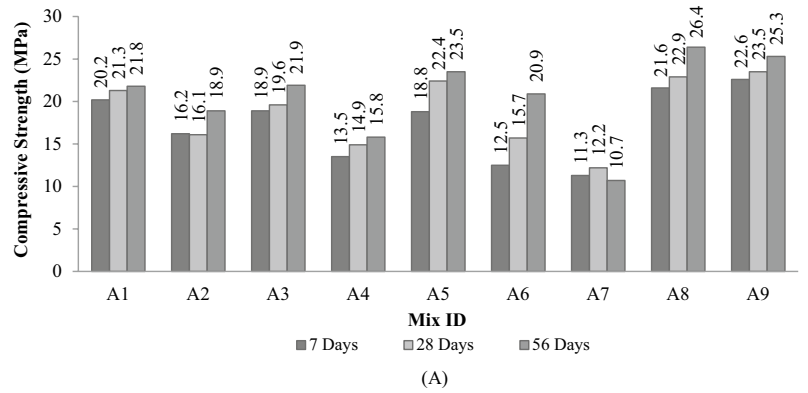


Fig. 10 (continued)

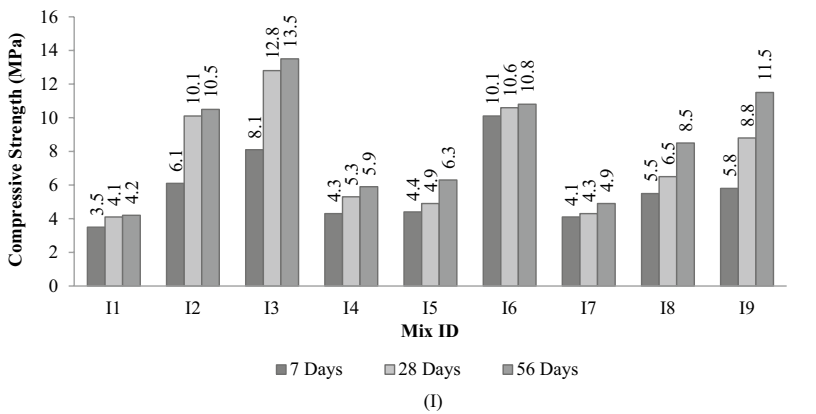
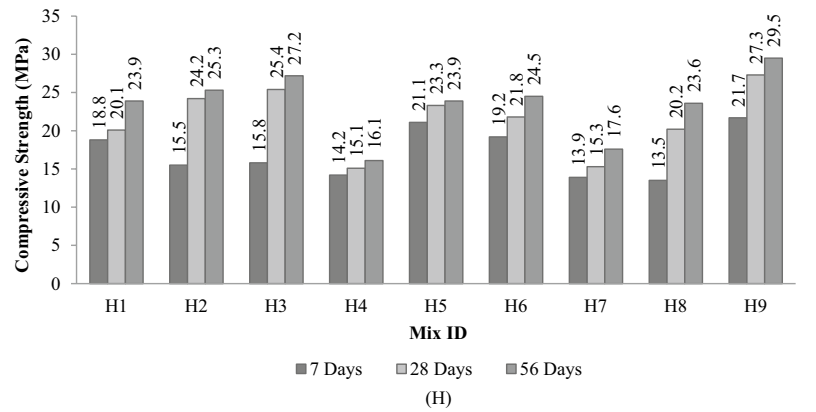
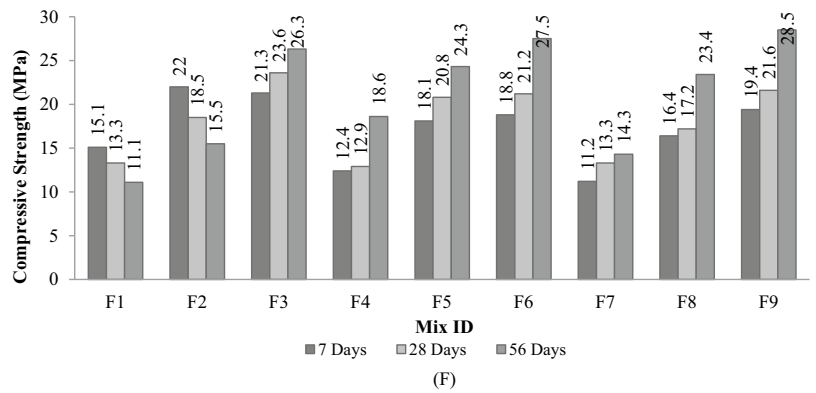
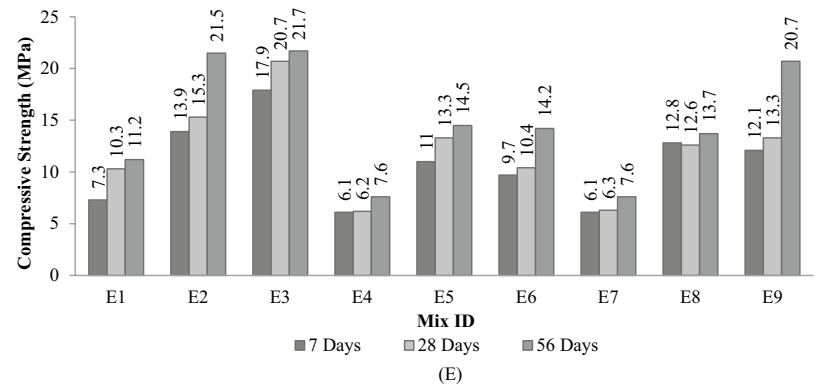
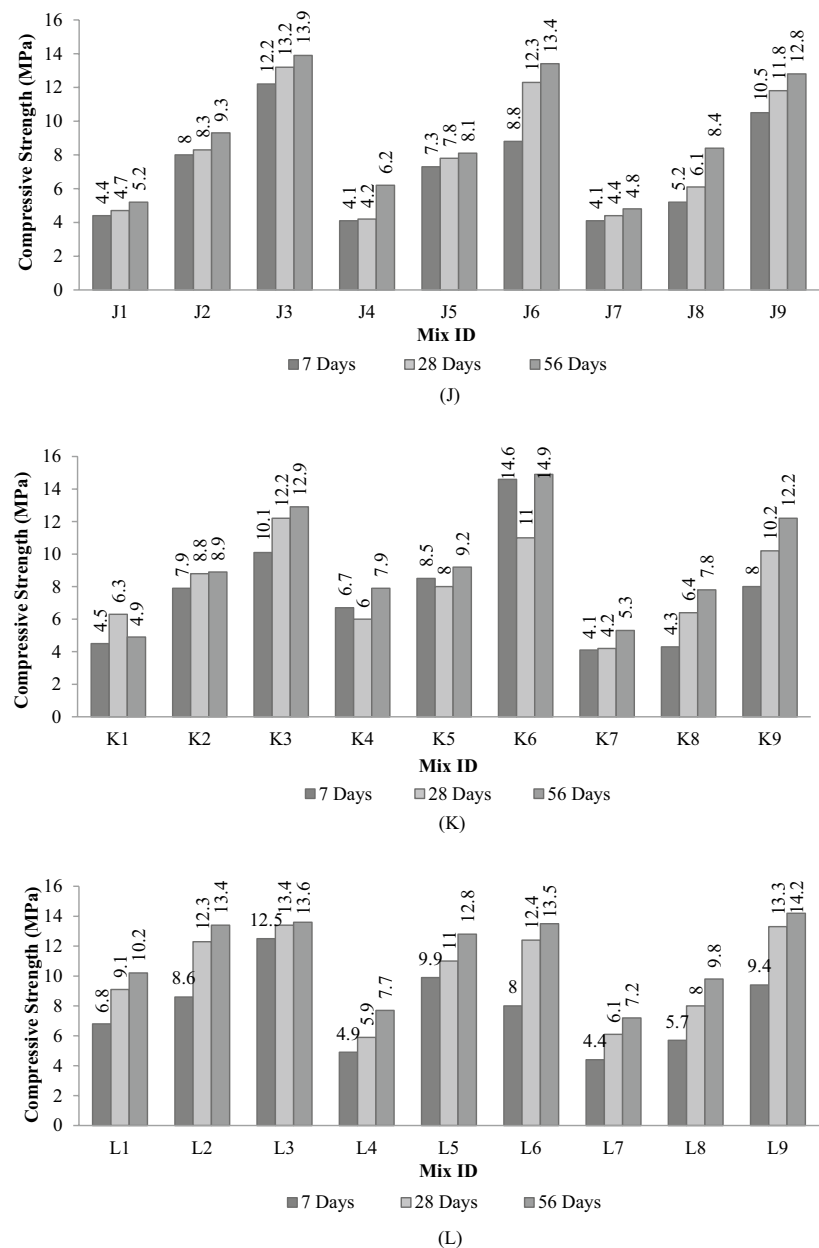


Fig. 10 (continued)



curing for different alkali concentrations, and the results are presented in Fig. 11A–C. Figure 11A–C are representing 1:2, 1:5, and 1:8 mix proportions of AASM for different alkali activator combinations.

#### 4.5 Discussion on mechanical properties of AASM

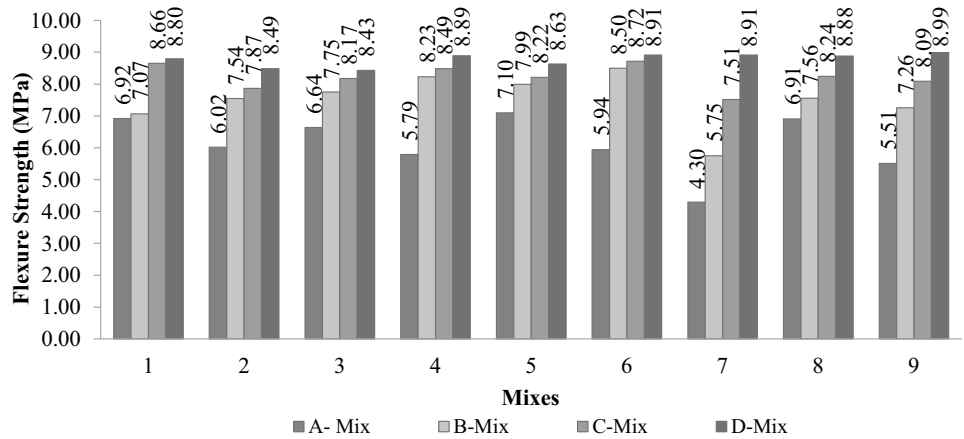
From Figs. 10A–L and 11A–C the compressive strength results correlate with the flexural strength results. The mechanical properties of AASM prepared with different combinations of mix proportions, alkali binder ratio, different molarities of NaOH, different concentrations of  $\text{Na}_2\text{SiO}_3$ , and different ages of curing are discussed below.

#### 4.6 Effect of mix proportion

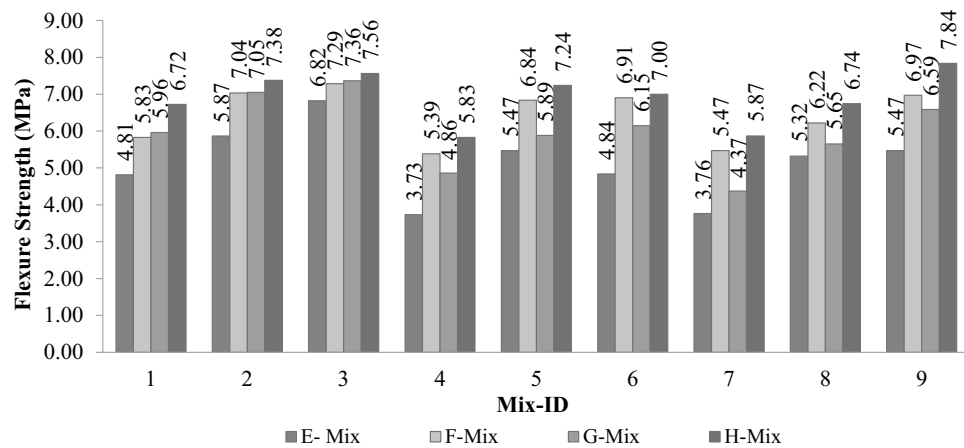
From Figs. 10A–L and 11A–C it is observed clearly, that the 1:2 mix proportion is producing high compressive strength and flexure strength values compared to the 1:5 mix proportion and 1:8 mix proportion. For a 1:2 mix of AASM of 19 M of NaOH and 50% of  $\text{Na}_2\text{SiO}_3$  Maximum compressive strength value of 41.6 MPa is observed after 56 days of curing and a maximum flexure strength value of 8.99 MPa is observed after 28 days of curing. The mix proportion of 1:8 exhibited very low compressive and flexure strength values.



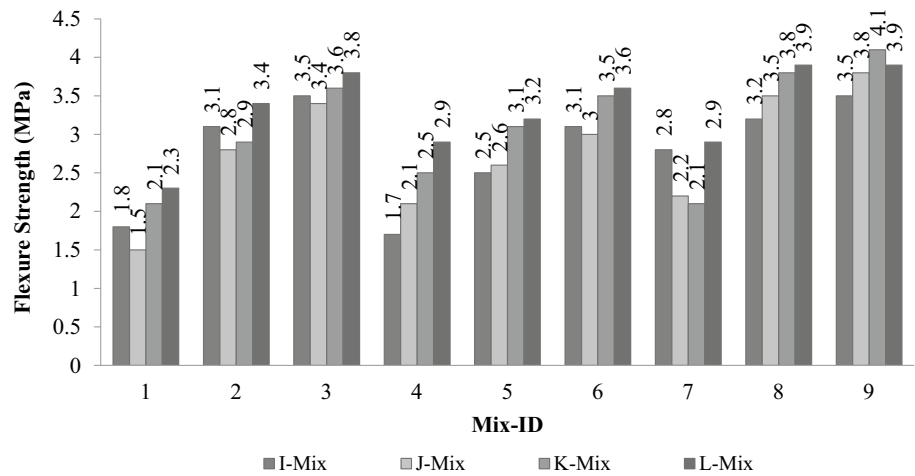
**Fig. 11** **A** Flexure strengths of AASM of 1:2 mix and 9 M to 19 M of NaOH. **B** Flexure strengths of AASM of 1:5 mix and 9 M to 19M of NaOH. **C** Flexure strengths of AASM of 1:8 mix and 9 M to 19M of NaOH



(A)



(B)



(C)

### 4.7 Effect of alkali binder ratio

For alkali binder ratios of 0.5, 0.65, and 0.8, as the alkali binder ratio increases, the compressive strength and flexure strengths of AASM also increase. The alkali binder

ratio of 0.8 produces a maximum compressive strength of 41.6 MPa and Flexural strength of 8.99 MPa. The alkali binder ratio of 0.5 produces the lowest compressive strength of 3.5 MPa and flexure strength of 2.04 MPa. The alkali binder ratio does not significantly affect the 50%

concentration of  $\text{Na}_2\text{SiO}_3$  compared to 20% and 35% concentrations of  $\text{Na}_2\text{SiO}_3$ .

#### 4.8 Effect of molarity of NaOH

For the considered molarities of 9 M, 13 M, 16 M, and 19 M of NaOH, the results show that the higher the molarity of NaOH is, the higher the strength gain of AASM. 19 molar NaOH has higher compressive and flexure strength values compared to other lower molarities. In each molarity of NaOH, as the concentration of  $\text{Na}_2\text{SiO}_3$  increases, the compressive and flexure strengths of AASM also increase.

#### 4.9 Effect of percentage concentration of $\text{Na}_2\text{SiO}_3$

For the considered concentrations of 20%, 35%, and 50% of  $\text{Na}_2\text{SiO}_3$ , the results show higher the concentration of  $\text{Na}_2\text{SiO}_3$ , higher is the strength gain of AASM. 50% concentration of  $\text{Na}_2\text{SiO}_3$  has higher compressive and flexure strength values compared to other lower concentrations of  $\text{Na}_2\text{SiO}_3$ . For a 20% concentration of  $\text{Na}_2\text{SiO}_3$  in a 1:2 mix proportion with a 0.5 alkali binder ratio, higher strength values are observed compared to alkali binder ratios of 0.65 and 0.8.

#### 4.10 Effect of age on compressive strength

In All mixes of AASM, from Fig. 10A–L the compressive strengths are increasing with age and it is observed that in 7 days AASM gains strength of 75–85% of strength to the total strength attained in 56 days and in 28 days AASM gains strength of 87–97% to the total strength attained in 56 days. The gaining of strength with age is increasing with the molarity of NaOH. For 9 M of NaOH AASM gains the strength of 90% in 7 days to the total strength attained in 56 days. This represents the lower molarity of NaOH (9 M) in AASM has insufficient alkali in mortar could not gain strength after 7 days. For the high molarity of NaOH, the

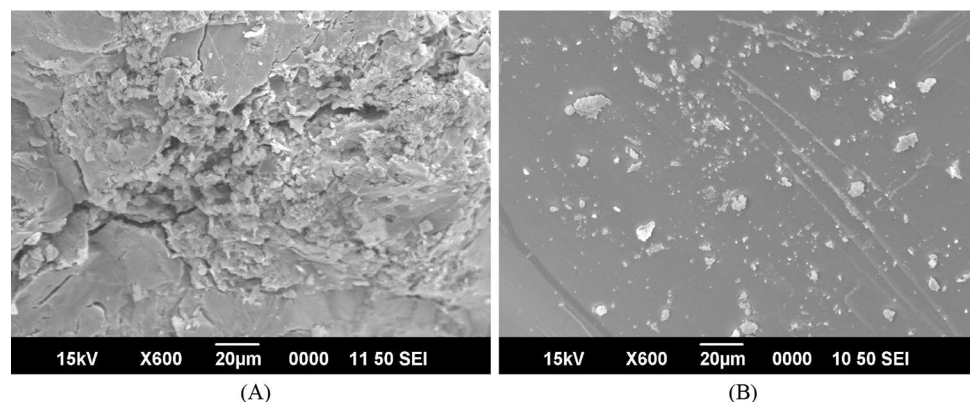
gaining of strength is more after 7 days due to the presence of more alkali for further reaction.

#### 4.11 SEM and EDX analysis

The microstructural analysis is carried out for the samples of low compressive strength (3.5 MPa) of AASM mix (I1) and high compressive strength (41.6 MPa) of AASM mix (D9). To study the morphology of AASM, Scanning Electron Microscope (SEM) analysis is conducted, and to study the elemental variability of AASM, an Energy Dispersive X-ray (EDX) analysis is carried out [70]. Figure 12A, B represent SEM images of resolution 20  $\mu\text{m}$  of I1 mix and D9 mix of AASM. Figure 13A, B represent EDX analysis images of the I1 mix and D9 mix of AASM.

The SEM image (Fig. 12A) of the I1 mix (1:8 mix, 9 M of NaOH, 20% of  $\text{Na}_2\text{SiO}_3$ , 0.5 and 7 days of ambient curing) shows very poor microstructure with the presence of more voids. The EDX analysis (Fig. 13A and Table 8) confirms the presence of more unreacted silica. For 7 days of ambient curing, only a certain amount of silica has participated in alkali activation with alkali so there is no proper binding material formed like Calcium-Alumino-Silicate Hydrate (CASH) and Sodium-Alumino-Silicate Hydrate (NASH) [18, 32]. The SEM image (Fig. 12B) of the D9 mix (1:2 mix, 19 M NaOH, 50% of  $\text{Na}_2\text{SiO}_3$ , 0.8 of A/B, and for 56 days) shows fully activated GGBS and SF with denser microstructure. The EDX analysis (Fig. 13B and Table 8) confirming the 3.46 Si/Al ratio, 2.72 Si/Na ratio, and 1.14 Si/Ca ratio represents reacted silica with Al, Na, and Ca confirming the formation of primary products like CASH and NASH and other secondary strong bond compounds [33]. Because of the formation of these strong compounds D9 mix of AASM for 56 days produces maximum compressive strength.

**Fig. 12** A SEM image for I1 mix of AASM. B SEM image for D9 mix of AASM



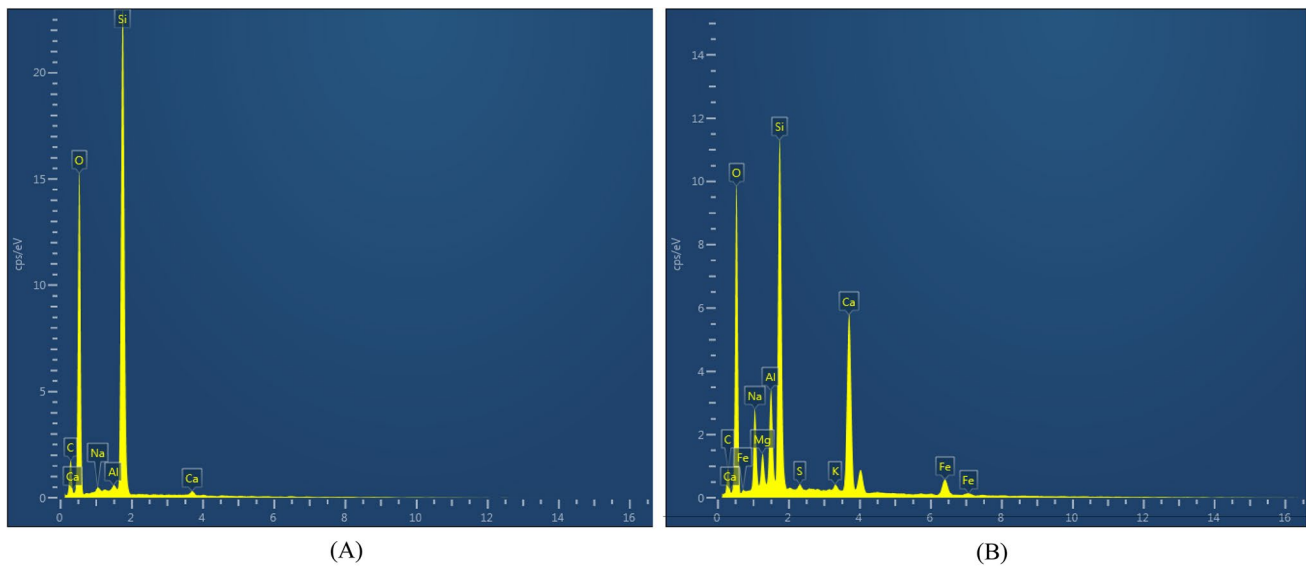


**Fig. 13** **A** EDX analysis for I1 mix of AASM. **B** EDX analysis for D9 mix of AASM

**Table 8** Atomic % I1 and D9 AASM mixes

Element	I1 mix wt%	D9 mix wt%
C	17.56	11.73
O	48.85	47.23
Na	0.34	5.19
Mg	0	1.7
Al	0.27	4.08
Si	32.23	14.1
S	0	0.27
K	0	0.37
Ca	0.75	12.37
Fe	0	2.95

## 5 Conclusions and recommendations

Based on experimental work in the scope reported in this study, the following conclusions are drawn.

Alkali Activated Slag Mortar developed with a binder 80% of GGBS and 20% of SF, with quartz sand exhibiting good performance at ambient air curing. An addition of 5% of gypsum is required for AASM to control setting time. The alkali activators influence the % of water absorption, and the rich mix has a lower % water absorption representing the presence of fewer pores in the mix. The workability of AASM is influenced by alkali activators, as the concentration of  $\text{Na}_2\text{SiO}_3$  increasing, the workability is decreasing, and as the molarity of NaOH increases the workability also increases. The rich mix 1:2 represents higher binder content resulting in higher

compressive and flexure strengths. High alkalinity to the binder ( $A/B=0.8$ ) ratio results in high strengths of AASM. A higher molar (19 M) of NaOH results in higher compressive and flexure strengths in AASM. The gaining of strength with age is more for higher molar NaOH compare to low molar NaOH due to the presence of more alkali for alkali activation. The performance of AASM is good at a 35% concentration of  $\text{Na}_2\text{SiO}_3$ . The compressive strength for 13 M, 16 M, and 19 M of NaOH increases with the increase in age until 56 days in all mixes of AASM. The flexural strength results correlate with the compressive strength results. Among all mixes of AASM, D9 mix (1:2 mix, 19 M NaOH, 50% of  $\text{Na}_2\text{SiO}_3$ , 0.8 of A/B) gives high compressive and flexure strength results, and I1 mix (1:8 mix, 9 M of NaOH, 20% of  $\text{Na}_2\text{SiO}_3$ , 0.5 of A/B) gives lowest compressive and flexure strength results. The SEM and EDX of the D9 mix for 56 days confirmed the formation of CASH and NASH and other secondary strong bond compounds resulting in a dense microstructure of AASM with high compressive strength.

This paper presents the detailed methodology for developing the GGBS and SF based AASM mixes under ambient air curing conditions which can be utilized for the manufacturing of bricks and plastering works. As AASM has high early age compressive strengths, it can be used in structural repairs as filler. As AASM is gaining strength in [ambient air curing](#), this AASM/AASC is very good construction material for the areas where water is scarce on earth. Since the AASM mixes contribute high compressive strength which can be opted in mass concreting works. However, a further experimental study is required for practical usage of alkali activators for mass concrete works, and to assess the

efficiency of AASM in the RC members. So AASM is a very good construction material, the utilization of AASM in the construction industry leads to a reduction of usage of cement content, which can ultimately lead to a reduction of the carbon footprint on the earth.

**Acknowledgements** The authors would like to acknowledge the STIC Kochi University, Kochi 682 022, Kerala, India for SEM and EDX data of AASC.

**Funding** This research received no specific grant from any funding agency from public, commercial or not-for-profit sectors.

## Declarations

**Conflict of interest** The Authors declare that there is no conflict of interest.

## References

- Kurtis KE (2015) Innovations in cement-based materials: Addressing sustainability in structural and infrastructure applications. *MRS Bull* 40:1102–1108. <https://doi.org/10.1557/mrs.2015.279>
- Hardjito D, Rangan BV (2005) Development and properties of low-calcium fly ash based geopolymer low-calcium fly ash-based geopolymer concrete by Faculty of Engineering Curtin University of Technology. *Aust Univ Technol Perth* 48
- Ali MB, Saidur R, Hossain MS (2011) A review on emission analysis in cement industries. *Renew Sustain Energy Rev* 15:2252–2261. <https://doi.org/10.1016/j.rser.2011.02.014>
- Costa FN, Ribeiro DV (2020) Reduction in CO<sub>2</sub> emissions during production of cement, with partial replacement of traditional raw materials by civil construction waste (CCW). *J Clean Prod* 276:123302. <https://doi.org/10.1016/j.jclepro.2020.123302>
- Srivastava V, Imam A, Mehta PK, Tripathi MK, Ash F (2018) Supplementary cementitious materials in construction—an attempt to reduce CO<sub>2</sub> emission. *J Nano Technol* 7:31–35. <https://doi.org/10.13074/jent.2018.06.182306>
- Asa E, Shrestha M, Baffoe-Twum E, Awuku B (2020) Development of sustainable construction material from fly ash class C. *J Eng Des Technol* 18:1615–1640. <https://doi.org/10.1108/JEDT-06-2019-0156>
- Kanamarlapudi L, Jonalagadda KB, Jagarapu DCK, Eluru A (2020) Different mineral admixtures in concrete: a review. *SN Appl Sci* 2:1–10. <https://doi.org/10.1007/s42452-020-2533-6>
- Huynh TP, Nguyen DT, Phan TD, Ho NT, Bui PT, Nguyen MH (2021) Evaluation of mechanical strength and durability characteristics of eco-friendly mortar with cementitious additives. *J Appl Sci Eng* 24:541–552. [https://doi.org/10.6180/jase.202108\\_24\(4\).0010](https://doi.org/10.6180/jase.202108_24(4).0010)
- Sharma R (2021) Effect of wastes and admixtures on compressive strength of concrete. *J Eng Des Technol* 19:219–244. <https://doi.org/10.1108/JEDT-01-2020-0031>
- Kong DLY, Sanjayan JG (2010) Effect of elevated temperatures on geopolymer paste, mortar and concrete. *Cem Concr Res* 40:334–339. <https://doi.org/10.1016/j.cemconres.2009.10.017>
- Ismail N, Mansour M, El-Hassan H (2017) Development of a low-cost cement free polymer concrete using industrial by-products and dune sand. *MATEC Web Conf* 120:1–8. <https://doi.org/10.1051/mateconf/201712003005>
- Xu H, Van Deventer JSJ (2000) The geopolymerisation of aluminosilicate minerals. *Int J Miner Process* 59:247–266. [https://doi.org/10.1016/S0301-7516\(99\)00074-5](https://doi.org/10.1016/S0301-7516(99)00074-5)
- Davidovits J (1994) Properties of geopolymer cements. In: First international conference on alkaline cement concrete, pp 131–149
- Mohamed O (2018) Durability and compressive strength of high cement replacement ratio self-consolidating concrete. *Buildings*. <https://doi.org/10.3390/buildings8110153>
- Revilla-Cuesta V, Skaf M, Serrano-López R, Ortega-López V (2021) Models for compressive strength estimation through non-destructive testing of highly self-compacting concrete containing recycled concrete aggregate and slag-based binder. *Constr Build Mater*. <https://doi.org/10.1016/j.conbuildmat.2021.122454>
- Ajith G, Shanmugasundaram N, Praveenkumar S (2021) Effect of mineral admixtures and manufactured sand on compressive strength of engineered cementitious composite. *J Build Rehabil* 6:38. <https://doi.org/10.1007/s41024-021-00137-y>
- Revilla-Cuesta V, Skaf M, Santamaría A, Hernández-Bagaces JJ, Ortega-López V (2021) Temporal flowability evolution of slag-based self-compacting concrete with recycled concrete aggregate. *J Clean Prod*. <https://doi.org/10.1016/j.jclepro.2021.126890>
- Revilla-Cuesta V, Skaf M, Santamaría A, Ortega-López V, Manso JM (2021) Assessment of longitudinal and transversal plastic behavior of recycled aggregate self-compacting concrete: a two-way study. *Constr Build Mater*. <https://doi.org/10.1016/j.conbuildmat.2021.123426>
- Mohamed OA (2019) A review of durability and strength characteristics of alkali-activated slag concrete. *Materials (Basel)*. <https://doi.org/10.3390/ma12081198>
- Cheah CB, Chung KY, Ramli M, Lim GK (2016) The engineering properties and microstructure development of cement mortar containing high volume of inter-grinded GGBS and PFA cured at ambient temperature. *Constr Build Mater* 122:683–693. <https://doi.org/10.1016/j.conbuildmat.2016.06.105>
- Bellum RR (2021) Influence of anti-washout admixtures on the strength and microstructural characteristics of geopolymer concrete. *J Build Rehabil* 6:35. <https://doi.org/10.1007/s41024-021-00129-y>
- Revilla-Cuesta V, Skaf M, Espinosa AB, Ortega-López V (2021) Multi-criteria feasibility of real use of self-compacting concrete with sustainable aggregate, binder and powder. *J Clean Prod*. <https://doi.org/10.1016/j.jclepro.2021.129327>
- Mathew BJ, Sudhakar M, Natarajan C (2013) Strength, economic and sustainability characteristics of coal ash—GGBS based geopolymer concrete. *Int J Comput Eng Res* 3:207–212
- Zhang P, Zheng Y, Wang K, Zhang J (2018) A review on properties of fresh and hardened geopolymer mortar. *Compos Part B Eng* 152:79–95. <https://doi.org/10.1016/j.compositesb.2018.06.031>
- Hafez H, Kassim D, Kurda R, Silva RV, de Brito J (2021) Assessing the sustainability potential of alkali-activated concrete from electric arc furnace slag using the ECO2 framework. *Constr Build Mater* 281:122559. <https://doi.org/10.1016/j.conbuildmat.2021.122559>
- Li C, Sun H, Li L (2010) A review: the comparison between alkali-activated slag (Si + Ca) and metakaolin (Si + Al) cements. *Cem Concr Res* 40:1341–1349. <https://doi.org/10.1016/j.cemconres.2010.03.020>
- Shekhawat P, Sharma G, Singh RM (2020) Durability analysis of eggshell powder–flyash geopolymer composite subjected to wetting–drying cycles. *J Eng Des Technol* 18:2043–2060. <https://doi.org/10.1108/JEDT-03-2020-0075>
- Srinivasan K, Sivakumar A (2013) Geopolymer binders: a need for future concrete construction. *ISRN Polym Sci* 2013:1–8. <https://doi.org/10.1155/2013/509185>



29. Davidovits J (1985) Early high-strength mineral polymer, United States Patent
30. Davidovits J (1982) Mineral polymers and methods of making them. US Pat 1–6
31. Sisol M, Kudelas D, Marcin M, Holub T, Varga P (2019) Statistical evaluation of mechanical properties of slag based alkali-activated material. *Sustain*. <https://doi.org/10.3390/su11215935>
32. De Vargas AS, Dal Molin DCC, Vilela ACF, Da SFJ, Pavão B, Veit H (2011) The effects of  $\text{Na}_2\text{O}/\text{SiO}_2$  molar ratio, curing temperature and age on compressive strength, morphology and microstructure of alkali-activated fly ash-based geopolymers. *Cem Concr Compos* 33:653–660. <https://doi.org/10.1016/j.cemcom.2011.03.006>
33. Kastiukas G, Zhou X, Castro-Gomes J, Huang S, Saafi M (2015) Effects of lactic and citric acid on early-age engineering properties of Portland/calcium aluminate blended cements. *Constr Build Mater* 101:389–395. <https://doi.org/10.1016/j.conbuildmat.2015.10.054>
34. Garcia-Lodeiro I, Palomo A, Fernández-Jiménez A (2015) An overview of the chemistry of alkali-activated cement-based binders. Woodhead Publishing Limited, Sawston
35. Puertas F, Palacios M, Manzano H, Dolado JS, Rico A, Rodríguez J (2011) A model for the C-A-S-H gel formed in alkali-activated slag cements. *J Eur Ceram Soc* 31:2043–2056. <https://doi.org/10.1016/j.jeurceramsoc.2011.04.036>
36. Palomo A, Grutzeck MW, Blanco MT (1999) Alkali-activated fly ashes: a cement for the future. *Cem Concr Res* 29:1323–1329. [https://doi.org/10.1016/S0008-8846\(98\)00243-9](https://doi.org/10.1016/S0008-8846(98)00243-9)
37. Markandeya Raju P, Lakshmi V, Santosh Kumar K (2021) Seasonal effect on compressive strength of ambient cured, nominal mix proportioned alkali-activated slag concrete. In: IOP conference series: materials science and engineering. IOP Publishing Ltd
38. Çevik A, Alzeebaree R, Humur G, Niş A, Gülşan ME (2018) Effect of nano-silica on the chemical durability and mechanical performance of fly ash based geopolymer concrete. *Ceram Int* 44:12253–12264. <https://doi.org/10.1016/j.ceramint.2018.04.009>
39. Nath P, Sarker PK (2014) Effect of GGBFS on setting, workability and early strength properties of fly ash geopolymer concrete cured in ambient condition. *Constr Build Mater* 66:163–171. <https://doi.org/10.1016/j.conbuildmat.2014.05.080>
40. Okoye FN, Durgaprasad J, Singh NB (2015) Mechanical properties of alkali activated flyash/kaolin based geopolymer concrete. *Constr Build Mater* 98:685–691. <https://doi.org/10.1016/j.conbuildmat.2015.08.009>
41. Gopal KM, Kiran BN (2013) Investigation on behaviour of fly ash based geopolymer concrete in acidic environment. *Int J Mod Eng Res* 3:580–586
42. Yuan XH, Chen W, Lu ZA, Chen H (2014) Shrinkage compensation of alkali-activated slag concrete and microstructural analysis. *Constr Build Mater* 66:422–428. <https://doi.org/10.1016/j.conbuildmat.2014.05.085>
43. Fattah KP, Al-Tamimi AK, Hamweyah W, Iqbal F (2017) Evaluation of sustainable concrete produced with desalinated reject brine. *Int J Sustain Built Environ* 6:183–190. <https://doi.org/10.1016/j.ijbs.2017.02.004>
44. Jindal BB (2019) Investigations on the properties of geopolymer mortar and concrete with mineral admixtures: a review. *Constr Build Mater* 227:116644. <https://doi.org/10.1016/j.conbuildmat.2019.08.025>
45. Okoye FN, Durgaprasad J, Singh NB (2016) Effect of silica fume on the mechanical properties of fly ash based-geopolymer concrete. *Ceram Int* 42:3000–3006. <https://doi.org/10.1016/j.ceramint.2015.10.084>
46. Dave N, Sahu V, Misra AK (2020) Development of geopolymer cement concrete for highway infrastructure applications. *J Eng Des Technol* 18:1321–1333. <https://doi.org/10.1108/JEDT-10-2019-0263>
47. Pavithra P, Srinivasula Reddy M, Dinakar P, Hanumantha Rao B, Satpathy BK, Mohanty AN (2016) Effect of the  $\text{Na}_2\text{SiO}_3/\text{NaOH}$  ratio and NaOH molarity on the synthesis of fly ash-based geopolymer mortar. *Geo-Chicago*. <https://doi.org/10.1061/9780784480151.034>
48. Markandeya Raju P, Lakshmi V, Santosh Kumar K (2021) Seasonal effect on compressive strength of ambient cured, nominal mix proportioned alkali-activated slag concrete. *IOP Conf Ser Mater Sci Eng*. <https://doi.org/10.1088/1757-899X/1025/1/012026>
49. Asa E, Anna AS, Baffoe-Twum E (2019) An investigation of mechanical behavior of concrete containing crushed waste glass. *J Eng Des Technol* 17:1285–1303. <https://doi.org/10.1108/JEDT-01-2019-0020>
50. Donza H, Cabrera O, Irassar EF (2002) High-strength concrete with different fine aggregate. *Cem Concr Res* 32:1755–1761. [https://doi.org/10.1016/S0008-8846\(02\)00860-8](https://doi.org/10.1016/S0008-8846(02)00860-8)
51. Mosaberpanah MA, Eren O (2017) Effect of quartz powder, quartz sand and water curing regimes on mechanical properties of UHPC using response surface modelling. *Adv Concr Constr* 5:481–492. <https://doi.org/10.12989/acc.2017.5.5.481>
52. Falah M, Obenaus-Emler R, Kinnunen P, Illikainen M (2020) Effects of activator properties and curing conditions on alkali-activation of low-alumina mine tailings. *Waste Biomass Valoriz* 11:5027–5039. <https://doi.org/10.1007/s12649-019-00781-z>
53. Humad AM, Provis JL, Cwirzen A (2019) Effects of curing conditions on shrinkage of alkali-activated high-MgO Swedish slag concrete. *Front Mater*. <https://doi.org/10.3389/fmats.2019.00287>
54. Chi M (2012) Effects of dosage of alkali-activated solution and curing conditions on the properties and durability of alkali-activated slag concrete. *Constr Build Mater* 35:240–245. <https://doi.org/10.1016/j.conbuildmat.2012.04.005>
55. More P, Kishanrao P (2013) Design of geopolymer concrete. Prof. more Pratap Kishanrao. *Int J Innov Res Sci Eng Technol* 2:1841–1844
56. Patil S V., Karikatti VB, Chitawadagi M (2018) Granulated blast-furnace slag (GGBS) based geopolymer concrete—review concrete—review. *Int J Adv Sci Eng* 5:879. <https://doi.org/10.29294/ijase.5.1.2018.789-885>
57. Hashempour M, Samani AA, Heidari A (2021) Essential improvements in gypsum mortar characteristics. *Int J Eng Trans B Appl* 34:319–325. <https://doi.org/10.5829/IJE.2021.34.02B.03>
58. Herliati SA, Dyah Puspita A, Puput Dwi R, Salasa A (2021) Optimization of gypsum composition against setting time and compressive strength in clinker for PCC (Portland Composite Cement). *IOP Conf Ser Mater Sci Eng* 1053:012116. <https://doi.org/10.1088/1757-899x/1053/1/012116>
59. Perry S, Perry RH, Green DW, Maloney JO (2000) Perry's chemical engineers' handbook
60. IS 2250-1981 (Reaffirmed 2000) Indian Standard code of Practice for preparation and use of Masonry Mortar. Bureau of Indian Standards, New Delhi
61. IS 4031 (Part 6)-1988 (Reaffirmed 2005) Methods of physical tests for hydraulic cement. Bureau of Indian Standards, New Delhi
62. American Society for Testing and Materials: Standard Test Method for Flexural Strength of Hydraulic Cement Mortars. *ANSI/ASTM C 348-80*, Philadelphia, pp 241–245
63. Phoo-Ngernkham T, Maegawa A, Mishima N, Hatanaka S, Chindaprasit P (2015) Effects of sodium hydroxide and sodium silicate solutions on compressive and shear bond strengths of FA-GGBFS geopolymer. *Constr Build Mater* 91:1–8. <https://doi.org/10.1016/j.conbuildmat.2015.05.001>



64. IS 10080-1982 (Reaffirmed 2004) Indian standard specification for vibration machine. Bureau of Indian Standards, New Delhi
65. Fang G, Ho WK, Tu W, Zhang M (2018) Workability and mechanical properties of alkali-activated fly ash-slag concrete cured at ambient temperature. *Constr Build Mater* 172:476–487. <https://doi.org/10.1016/j.conbuildmat.2018.04.008>
66. Ramamurthy K, Manikandan R (2006) Workability and strength of masonry mortars with high volume Class-C fly ash. *Mason Int Cl*:89–96
67. IS 5512-1983(Reaffirmed 2004) Specification for flow table for use in tests of hydraulic cements and pozzolanic materials. New Delhi
68. Kubica J, Galman I (2022) Investigations on flexural and compressive strengths of mortar dedicated to clinker units—influence of mixing water content and curing time. *Materials* (Basel). <https://doi.org/10.3390/ma15010347>
69. Aho I, Ndububa E (2015) Compressive and flexural strength of cement mortar stabilized with raffia palm fruit peel (RPEP). *Glob J Eng Res* 14:1. <https://doi.org/10.4314/gjer.v14i1.1>
70. Ng C, Alengaram UJ, Wong LS, Mo KH, Jumaat MZ, Ramesh S (2018) A review on microstructural study and compressive strength of geopolymer mortar, paste and concrete. *Constr Build Mater* 186:550–576. <https://doi.org/10.1016/j.conbuildmat.2018.07.075>

**Publisher's Note** Springer Nature remains neutral with regard to jurisdictional claims in published maps and institutional affiliations.

Springer Nature or its licensor holds exclusive rights to this article under a publishing agreement with the author(s) or other rightsholder(s); author self-archiving of the accepted manuscript version of this article is solely governed by the terms of such publishing agreement and applicable law.